Available online at www.sciencedirect.com
ScienceDirect
Comput. Methods Appl. Mech. Engrg. 196 (2007) 1193–1202
Computer methods in applied mechanics and engineering
www.elsevier.com/locate/cma

On spurious velocities in incompressible flow problems with interfaces

Sashikumaar Ganesan [a], Gunar Matthies [b], Lutz Tobiska [a,*]

[a] Institut für Analysis und Numerik, Otto-von-Guericke-Universität Magdeburg, Postfach 4120, 39016 Magdeburg, Germany
[b] Fakultät für Mathematik, Ruhr-Universität Bochum, Universitätsstraße 150, 44780 Bochum, Germany

Received 3 January 2006; received in revised form 16 August 2006; accepted 24 August 2006

Abstract

We show that a non-physical velocity may appear in the finite element calculation of incompressible two-phase flows subjected to an external local force. There are different sources responsible for this phenomenon: approximation of the incompressibility constraint, the interface, and the local external force. Furthermore, we demonstrate that this non-physical velocity does not vanish with the expected order of convergence. We evaluate different concepts and give recommendations for a proper handling of this phenomenon.

Keywords: Incompressible flow; Two-phase flow; Interface; Finite elements

1. Introduction

Spurious velocities in incompressible flow problems have been observed in a number of papers, see, e.g., [1–5]. A typical situation is the one-phase Stokes flow

$$-\Delta u + \nabla p = f, \quad \nabla \cdot u = 0, \quad \text{in } \Omega, \quad u = 0 \quad \text{on } \Gamma_D,$$

under the influence of an external force. In case that f is the gradient of a scalar potential, $f = \nabla \Phi$, the (up to an additive constant for the pressure) unique solution becomes $u = 0$, $p = \Phi$. This property is in general not preserved by a discretisation scheme, i.e., the discrete velocities do not vanish. For a general external force it can be observed that the 'gradient part' may also produce a velocity field which pollutes the physical flow. This may result in serious problems in coupled flow problems, e.g., for thermically driven flows described by the Boussinesq equation [1,3]. Since the effect cannot be observed in a divergence-free setting, an early proposal to overcome this difficulty was to enrich the pressure space in order to make the remaining velocity space closer to the divergence-free subspace [1,2,6]. Nevertheless, in [3, Chapter 6] and [7] it has been shown that spurious velocities can appear in conforming as well as non-conforming finite element discretisations. An essential idea developed for a general external force is to calculate an approximate 'gradient part' and project it to the discrete pressure space [3,4]. For an extension and application of this idea which is related to the pressure separation in the Navier–Stokes equations, see also [8].

Local external forces appear in two-phase flows due to capillary forces at the interface of two immiscible fluids. In this case there are much more sources for producing spurious velocities: the approximation of the (unknown) interface, the approximation of the curvature in capillary forces, etc. In all these cases the dynamics depend strongly on the size of spurious velocities near the interface. In particular, unphysical movements of the interface could be generated by spurious velocities and could lead to a complete misinterpretation. Therefore, the main focus of this paper is to study the reasons for spurious velocities in incompressible flows with interfaces. Although our investigations are focused on finite element discretisations, the same phenomena can be observed in finite volume methods, e.g., see [5].

* Corresponding author.
E-mail addresses: ga.sashikumaar@mathematik.uni-magdeburg.de (S. Ganesan), Gunar.Matthies@ruhr-uni-bochum.de (G. Matthies), tobiska@mathematik.uni-magdeburg.de (L. Tobiska).
URLs: http://www.ruhr-uni-bochum.de/jpnum (G. Matthies), http://www-ian.math.uni-magdeburg.de/tobiska (L. Tobiska).

0045-7825/$ - see front matter © 2006 Elsevier B.V. All rights reserved.
doi:10.1016/j.cma.2006.08.018

The paper is organised as follows. In Section 2 we formulate a two-phase flow problem in equilibrium state which will serve as a test case for spurious velocities. We will describe finite element discretisations on interface adapted and non-adapted meshes, respectively. Special focus will be given to different approaches for discretising the local external force. We also discuss the birth of spurious velocities. Section 3 is devoted to the approximation of discontinuous functions on adapted and non-adapted meshes in one space dimensions by discontinuous and continuous functions, respectively. In Section 4 we perform several numerical tests. We investigate two different inf–sup stable finite element discretisations of second order on both adapted and non-adapted meshes. Next, we study the discretisation error of the approximated normal flux on the interface. For the best pair of finite elements on interface adapted meshes we finally evaluate the different discretisation approaches for the local external force. Based on the observed analytical and numerical results we give final conclusions.

2. Model problem and its discretisation

2.1. Problem description

We consider a two-dimensional stationary two-phase problem, that is, two immiscible liquids, occupying Ω_1 and Ω_2, are placed in a closed container Ω. We assume that Ω_1 is completely inside the liquid Ω_2, such that Ω_1 has no contact with the container boundaries. Furthermore, we neglect gravitational effects and assume that the system is in equilibrium. The simplest example of this type is given as follows: Let $\Omega = (-2,2)^2 \subset \mathbb{R}^2$, the container boundary $\Gamma_D = \partial\Omega$, Ω_1 be the circle with radius 1 around $(0,0)$, the interface $\Gamma_F = \partial\Omega_1$, and $\Omega_2 := \Omega\backslash(\Omega_1 \cup \Gamma_F)$, as shown in Fig. 1. We consider the stationary incompressible two-phase Stokes equations

$$\begin{aligned} &-\operatorname{div}\mathbb{T}(u,p) = 0 \quad \text{in } \Omega_1 \cup \Omega_2,\\ &\operatorname{div} u = 0 \quad \text{in } \Omega_1 \cup \Omega_2,\\ &u = 0 \quad \text{on } \Gamma_D,\\ &[|u|] = 0 \quad \text{on } \Gamma_F,\\ &t \cdot [|\mathbb{T}(u,p)|]n = 0 \quad \text{on } \Gamma_F,\\ &n \cdot [|\mathbb{T}(u,p)|]n = \sigma\mathscr{K} \quad \text{on } \Gamma_F, \end{aligned} \tag{1}$$

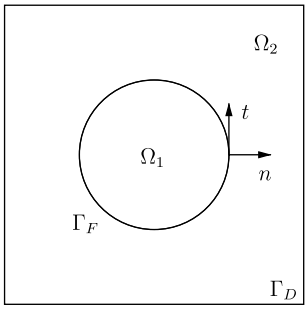

Fig. 1. Computational domain.

where u is the velocity, p the pressure, $\mathscr{K}$ the curvature of Γ_F, and σ the coefficient of the interfacial tension. The outer unit normal vector on Γ_F w.r.t. Ω_1 is denoted by n. Let t be the tangential unit vector on Γ_F obtained by a counterclockwise rotation of $\pi/2$ from n, as shown in Fig. 1. The stress tensor $\mathbb{T}(u,p)$ in Ω_k is given by

$$\mathbb{T}(u,p) = -p\mathbb{I} + 2\mu_k\mathbb{D}(u), \quad k = 1,2$$

with the dynamic viscosity μ_k of the respective liquids, the unit tensor $\mathbb{I}$, and the velocity deformation tensor $\mathbb{D}(u)$ whose entries are defined by

$$\mathbb{D}(u)_{ij} = \frac{1}{2}\left(\frac{\partial u_i}{\partial x_j} + \frac{\partial u_j}{\partial x_i}\right), \quad i,j = 1,2.$$

In Eq. (1), $[|\cdot|]$ denotes the jump across the interface Γ_F. For a piecewise smooth function w, we define its jump $[|w|]$ by

$$[|w|] := (w|_{\Omega_2})|_{\Gamma_F} - (w|_{\Omega_1})|_{\Gamma_F}.$$

Since our primary interest is to study the influence of different discretisations on spurious velocity, we use $\sigma = \mu_1 = \mu_2 = 1$ in our calculations. Furthermore, the solution of (1) is analytically known to be

$$u \equiv 0 \quad \text{in } \Omega, \qquad p = \begin{cases} \pi/16 - 1 & \text{in } \Omega_1,\\ \pi/16 & \text{in } \Omega_2. \end{cases} \tag{2}$$

Here, we have used that $\mathscr{K} = 1$ on Γ_F, the boundary of the unit circle.

Let $V := (H_0^1(\Omega))^2$ and $Q := L_0^2(\Omega)$ be the usual Sobolev spaces. The inner product in $L^2(\Omega)$, its vector-valued and tensor-valued versions is denoted by $(\cdot,\cdot)$, while the inner product in $L^2(\Gamma_F)$ and its vector-valued version is given by $\langle\cdot,\cdot\rangle$.

A weak formulation of problem (1) is obtained in the usual way. First, we multiply the partial differential equations by test functions $v \in V$ and $q \in Q$, respectively, and integrate over Ω. Then, after integrating by parts over the subdomains Ω_1 and Ω_2 separately, we can incorporate the boundary conditions which are not of Dirichlet type. In particular, the stress tensor term becomes

$$\begin{aligned} -(\operatorname{div}\mathbb{T}(u), v) &= 2(\mathbb{D}(u), \mathbb{D}(v)) - (p, \operatorname{div} v) - \langle v \cdot [|\mathbb{T}(u)|], n\rangle\\ &= 2(\mathbb{D}(u), \mathbb{D}(v)) - (p, \operatorname{div} v) - \langle \mathscr{K}, v \cdot n\rangle \end{aligned}$$

Hence, a weak formulation of problem (1) is given by

Find $(u,p) \in V \times Q$ such that

$$\begin{aligned} &2(\mathbb{D}(u), \mathbb{D}(v)) - (p, \operatorname{div} v) = \langle \mathscr{K}, v \cdot n\rangle \quad \forall v \in V,\\ &(q, \operatorname{div} u) = 0 \quad \forall q \in Q, \end{aligned} \tag{3}$$

which is a standard saddle-point problem.

2.2. Problem discretisation

We mainly focus to study the effects of different triangulations, (i.e., whether the interface is resolved by the mesh or not), different finite element discretisations (in particular, continuous and discontinuous approximation of the

pressure), and approximation of the curvature on spurious velocities.

To study the effects of the triangulation, we consider two families $\{\mathscr{T}_h^{(a)}\}$ and $\{\mathscr{T}_h^{(n)}\}$ of shape regular triangulations of Ω into (possibly curved) quadrilaterals. The family $\{\mathscr{T}_h^{(a)}\}$ contains interface adapted meshes, i.e., the interface Γ_F is resolved by the mesh. The second family $\{\mathscr{T}_h^{(n)}\}$ consists of meshes of rectangles which are aligned to the coordinate axes. Hence, the interface Γ_F cannot be resolved by these triangulations. For both families, a typical representative is shown in Fig. 2.

Furthermore, to study the effects of different finite element discretisations, two different types of discretisations which differ in their pressure approximations will be considered on triangulations of both families $\{\mathscr{T}_h^{(a)}\}$ and $\{\mathscr{T}_h^{(n)}\}$. The Taylor–Hood element Q_2/Q_1 uses a continuous pressure approximation while the element Q_2/P_1^{disc} approximates the pressure by discontinuous functions. In both cases, the spaces which are used for approximating the velocity and the pressure are denoted by V_h and Q_h, respectively. Note that both methods are conforming since we have $V_h \subset V$ and $Q_h \subset Q$. Furthermore, both discretisations fulfil the inf–sup stability condition, i.e., there exists a positive constant β independent of the discretisation parameter h such that

$$\inf_{q_h \in Q_h} \sup_{v_h \in V_h} \frac{(\operatorname{div} v_h, q_h)}{|v_h|_1 \|q_h\|_0} \geqslant \beta$$

holds true, see [9,10].

In the case of the interface adapted meshes from $\{\mathscr{T}_h^{(a)}\}$, two ways of interface representations are considered. For the first one, we assume that the interface is given only by the straight sides of the quadrilaterals at the interface Γ_F, while the second approach uses a second order approximation of the interface by isoparametric elements in order to take care of the curved interface. Since both the linear and second order approximations of the interface Γ_F are not smooth enough to calculate the curvature by an explicit formula, additional tools are needed to handle the curvature $\mathscr{K}$.

To study the effects of different curvature handling techniques, we shall consider three approaches for the curvature term $\langle \mathscr{K}, v \cdot n \rangle$ on the right-hand side of the first equation in (3). For the first one, we use the fact that the curvature $\mathscr{K}$ on the interface Γ_F of the unit circle is known to be 1.

However, in many practical applications, the interface position is not explicitly known, especially in instationary problems. Hence, the calculation of the exact curvature is not possible. Thus, we consider as a second approach the often used interpolated cubic spline to get an approximated curvature. The interpolated cubic spline is constructed from the discretised interface Γ_F. For the bilinear case, we just use the vertices on Γ_F, while for the isoparametric case, for each curved edge its midpoint which lies directly on Γ_F is additionally taken into account.

A third way to get rid of calculating the curvature is to use the Laplace–Beltrami operator for the curvature and then apply the integration by parts to the Laplace–Beltrami operator over the interface Γ_F. This technique of reducing the order of differentiation associated with the curvature term had already be employed in a paper by Ruschak [11] in the context of the finite element simulation of the surface tension dominated flows. Its formulation by means of the Laplace–Beltrami operator goes back to Dziuk [12,13] and was also used by Bänsch [14,15]. We will describe this approach which is based on differential geometry in more detail. Let U be an open set such that $\Gamma_F \subset U$. For a function $f : U \to \mathbb{R}$ we define its tangential derivative $\underline{\nabla} f$ as

$$\underline{\nabla} f := \nabla f - (n \cdot \nabla f) n.$$

By denoting $\delta_i f := (\underline{\nabla} f)_i = \partial_i f - (n \cdot \nabla f) n_i$, $i = 1, \ldots, d$, the Laplace–Beltrami operator $\underline{\Delta}$ applied to f is given by

$$\underline{\Delta} f := \sum_{i=1}^{d} \delta_i (\delta_i f).$$

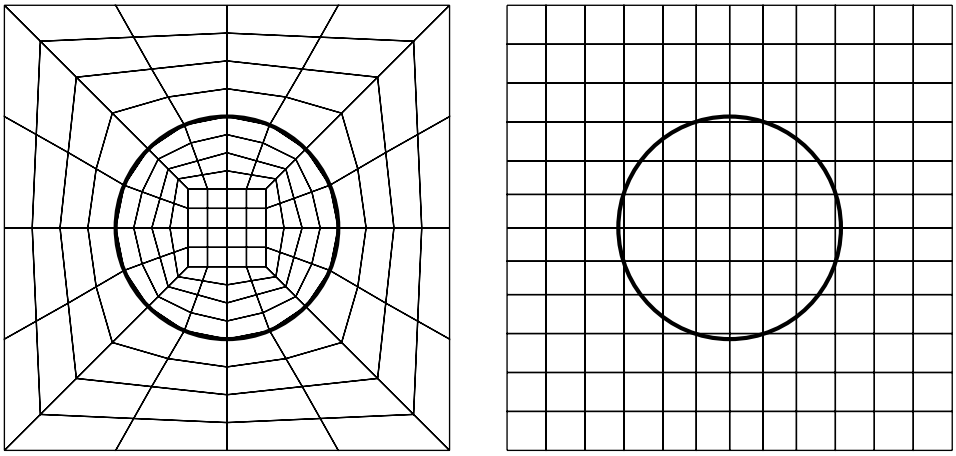

Fig. 2. Adapted (left) and non-adapted (right) meshes together with interface Γ_F.

Note that both the tangential derivative and the Laplace–Beltrami operator need formally values of f on U and not only on Γ_F, but the results depend only on the restriction of f to Γ_F. For vector-valued functions, the above definitions are applied component-wise. Since Γ_F is closed, the integration by parts

$$\langle f, \underline{\Delta} g\rangle = -\langle \underline{\nabla} f, \underline{\nabla} g\rangle$$

holds true on Γ_F for $f \in \mathscr{C}_0^2(U)$ and $g \in \mathscr{C}^2(U)$, see [16]. Furthermore, we have

$$\underline{\Delta}\mathrm{id}_{\Gamma_F} = \mathscr{K} n$$

where $\mathrm{id}_{\Gamma_F} : \Gamma_F \to \Gamma_F$ is the identity mapping on Γ_F, see [16]. Hence, the curvature term $\langle \mathscr{K}, v \cdot n\rangle$ can be replaced by $-\langle \underline{\nabla} i\mathrm{d}_{\Gamma_F}, \underline{\nabla} v\rangle$. Note that in this approach, only first order derivatives are needed to handle the curvature term.

The line integrals which occur for all meshes and different types of discretisations and different handling of the boundary were evaluated by means of an 11-point Gaussian quadrature formula which is exact for polynomials up to order 21.

2.3. Birth of spurious velocities

Since the weak solution of (3) is $(u,p) = (0,p)$, the fluid is in rest. We would like to have a numerical method which preserves this property, i.e., $u_h = 0$ should hold.

Let us introduce the spaces W and W_h of divergence-free and discretely divergence-free functions, respectively:

$$W = \{v \in V : (q, \operatorname{div} v) = 0 \quad \forall q \in Q\},$$
$$W_h = \{v_h \in V_h : (q_h, \operatorname{div} v_h) = 0 \quad \forall q_h \in Q_h\}.$$

The problem (3) is equivalent to the following weak formulation in the space W of divergence-free functions:

Find $u \in W$ such that

$$2(\mathbb{D}(u), \mathbb{D}(v)) = 0 \quad \forall v \in W,$$

since the boundary integral on the right-hand side vanishes due to the divergence theorem. Furthermore, the solution of this problem is $u = 0$ due to Korn's inequality and the homogeneous boundary conditions. If $W_h \subset W$ would hold then the approximation of the curvature term is not needed and the discrete problem results in

Find $u_h \in W_h$ such that

$$2(\mathbb{D}(u_h), \mathbb{D}(v_h)) = 0 \qquad \forall v_h \in W_h$$

with the solution $u_h = 0$. This is just what we wanted, namely $u = 0$ results in $u_h = 0$. However, in general it is expensive to construct divergence-free finite elements. For instance, one could choose the curl of C^1-elements.

Now we turn to the realistic situation in which $W_h \not\subset W$. After discretising (3) in $V_h \times Q_h$, our discrete problem reads:

Find $(u_h, p_h) \in V_h \times Q_h$ such that

$$\begin{aligned} &2(\mathbb{D}(u_h), \mathbb{D}(v_h)) - (p_h, \operatorname{div} v_h) = \langle \mathscr{K}_h, v_h \cdot n\rangle \quad \forall v_h \in V_h, \\ &(q_h, \operatorname{div} u_h) = 0 \quad \forall q_h \in Q_h. \end{aligned} \tag{4}$$

Here, the notation $\mathscr{K}_h$ has been used to indicate that the curvature term might be approximated in one of the ways described in Section 2.2.

In the case where the pressure solution p from (3) is in the discrete pressure space Q_h and the curvature term is exactly evaluated, we get by using $u \equiv 0$ and (3) with $v = u_h$

$$2\|\mathbb{D}(u_h)\|_0^2 = \langle \mathscr{K}_h, u_h \cdot n\rangle = \langle \mathscr{K}, u_h \cdot n\rangle = -(p, \operatorname{div} u_h) = 0, \tag{5}$$

i.e., $u_h = 0$ holds true due to Korn's inequality which is applicable since $V_h \subset V$. However, in general we have $p \notin Q_h$ or approximations of the curvature term are used. Then, the discrete solution u_h does not vanish identically, instead we have the error bound

$$|u_h|_1 \leqslant C\left(\inf_{q_h \in Q_h} \|p - q_h\|_0 + \sup_{v_h \in V_h} \frac{|\langle \mathscr{K}_h, v_h \cdot n\rangle - \langle \mathscr{K}, v_h \cdot n\rangle|}{|v_h|_1}\right), \tag{6}$$

where the second term is a consistency error introduced by the approximation of the curvature term. Thus, we see that the size of these *spurious velocities* depend on the approximation properties of both the pressure and the curvature term.

3. Approximation of discontinuous, piecewise smooth functions

For flow problems with interfaces, the pressure can exhibit jumps as it is the case in our test problem. In the following, we shall consider discontinuous approximations of functions which are only piecewise smooth on jump-adapted or jump-non-adapted meshes in one space dimension. The simplest example of a discontinuous, piecewise smooth function is $f : (-1,+1) \to \mathbb{R}$ given by $f(x) = \operatorname{sign}(x)$.

3.1. Discontinuous approximations on non-adapted meshes

Let P_0 denote the space of piecewise constant functions on $(-1,1)$. Let us assume that the jump of f at $x = 0$ appears in the cell $I = (-a,b)$, $a,\ b > 0$. Then, the best approximation $\varphi_h \in P_0$ of f is given by

$$\varphi_h(x) = \frac{b-a}{a+b}, \quad x \in I, \quad \varphi_h(x) = f(x) \quad \text{otherwise.}$$

Hence, the error estimate

$$\inf_{g_h \in P_0} \|f - g_h\|_0 = \|f - \varphi_h\|_0 = \sqrt{\frac{4ab}{a+b}} \tag{7}$$

is obtained. Since $h = a + b$, $a, b = \mathscr{O}(h)$ we have at least

$$\inf_{g_h \in P_0} \|f - g_h\|_0 = \mathcal{O}(\sqrt{h}).$$

Moreover, from (7) we see that in order to recover the optimal first order approximation for smooth functions, we have to resolve the jump by the mesh such that the shortest distance from the jump to a node of the mesh is of order 2, shortly

$$\min(a, b) = \mathcal{O}(h^2).$$

Let us consider now the space P_1^{disc} of discontinuous, piecewise linear functions. The jump of f at $x = 0$ is assumed again to appear in the cell $I = (-a, b)$, a, $b > 0$. Now, the best approximation $\varphi_h \in P_1^{\text{disc}}$ of f is given by

$$\varphi_h(x) = \begin{cases} \dfrac{12abx + (b-a)(a^2 - 4ab + b^2)}{(a+b)^3} & x \in I, \\ f(x) & \text{otherwise}, \end{cases}$$

which results in

$$\inf_{g_h \in P_1^{\text{disc}}} \|f - g_h\|_0 = \|f - \varphi_h\|_0 = \sqrt{\frac{4ab(a^2 - ab + b^2)}{(a+b)^3}}. \tag{8}$$

Again, we get at least

$$\inf_{g_h \in P_1} \|f - g_h\|_0 = \mathcal{O}(\sqrt{h}).$$

Now, in order to recover the optimal second order approximation for smooth functions, we see from (8) that we have to resolve the jump by the mesh much more accurate, namely

$$\min(a, b) = \mathcal{O}(h^4).$$

3.2. Continuous approximations on adapted and non-adapted meshes

In this section, we study the approximation of discontinuous functions by means of continuous functions. Let us first consider the case of a mesh which is not adapted to the jump of the function which should be approximated. Since the space P_1^{con} of continuous, piecewise linear functions is a subspace of the space P_1^{disc} of discontinuous, piecewise linear functions we have

$$\inf_{g_h \in P_1^{\text{con}}} \|f - g_h\|_0 \geqslant \inf_{g_h \in P_1^{\text{disc}}} \|f - g_h\|_0 = \sqrt{\frac{4ab(a^2 - ab + b^2)}{(a+b)^3}}.$$

Hence, we conclude that for getting the optimal second order approximation we have to resolve the jump by the mesh such that the shortest distance from the jump to a node of the mesh is of order 4, shortly

$$\min(a, b) = \mathcal{O}(h^4).$$

Now assume that a mesh node coincides with the position of the jump at $x = 0$. Let the two neighbouring elements be $(-a, 0)$ and $(0, b)$. Furthermore, we set $I = (-a, b)$. A short calculation gives

$$\inf_{g_h \in P_1^{\text{con}}} \|f - g_h\|_0 \geqslant \inf_{g_h \in P_1^{\text{con}}} \|f - g_h\|_{0,I} = \sqrt{\frac{ab}{a+b}} = \mathcal{O}(\sqrt{h})$$

with the best local approximation

$$\varphi_h|_I(x) = \begin{cases} \dfrac{3bx}{a(a+b)} + \dfrac{b-a}{a+b} & \text{if } x < 0, \\ \dfrac{3ax}{b(a+b)} + \dfrac{b-a}{a+b} & \text{if } x > 0. \end{cases}$$

This is even worse, showing that one should definitely avoid continuous approximations for discontinuous, piecewise smooth functions also in the case that the discontinuities are resolved by the mesh.

4. Numerical studies

4.1. Influence of the discretisation on spurious velocity

In this section, we will compare the numerically computed solutions for velocity and pressure of the different discretisations on the different meshes which are described in Section 2.2. We consider four cases

Case 0: isoparametric Q_2/P_1^{disc} on adapted meshes with given curvature,
Case 1: isoparametric Q_2/Q_1 on adapted meshes with given curvature,
Case 2: Q_2/Q_1 on non-adapted meshes with given curvature,
Case 3: Q_2/P_1^{disc} on non-adapted meshes with given curvature,

in our computations. The computational meshes are obtained by successively refining initial coarse meshes. The meshes generated after two refinement steps are shown in Fig. 2. Note that for the family $\{\mathcal{T}_h^{(a)}\}$ of interface adapted meshes, the interface Γ_F is taken into account during refinement by putting the newly generated midpoints of interface edges directly on Γ_F instead of putting them just on the straight edge.

Computations were performed up to level 7. The discretisations were solved by using the multiple discretisation multi-level solver, see [17]. For refinement level 4–7, the number of degrees of freedom for all four cases are given in Tables 1 and 2. The computations were carried out with the code MooNMD, see [18].

The modulus of the spurious velocity and the pressure for case 1 are shown in Fig. 3. The arrows in the left pictures indicate the direction of the spurious velocity only while the colour corresponds to its magnitude. Furthermore, we see from Fig. 3 that the pressure is piecewise constant in regions away from Γ_F. Fig. 4 shows the spurious velocities for case 2 and 3. The pressure pictures are not shown since the behaviour of the pressure in the cases 2 and 3 is very similar to the case 1. In the cases 1–3, the spurious velocities occur only near the interface region, see Figs. 3 and 4. Even in case 1 where the interface is resolved by the mesh, spurious

Table 1
Degrees of freedom for velocity and pressure in case 0 and 1

Level	Case 0			Case 1		
	Velocity	Pressure	Total	Velocity	Pressure	Total
4	18,562	6912	25,474	18,562	2337	20,899
5	73,986	27,648	101,634	73,986	9281	83,267
6	295,426	110,592	406,018	295,426	36,993	332,419
7	1,180,674	442,368	1,623,042	1,180,674	147,713	1,328,387

Table 2
Degrees of freedom for velocity and pressure in case 2 and 3

Level	Case 2			Case 3		
	Velocity	Pressure	Total	Velocity	Pressure	Total
4	18,818	2401	21,219	18,818	6912	25,730
5	74,498	9409	83,907	74,498	27,648	102,146
6	296,450	37,249	333,699	296,450	110,592	407,042
7	1,182,722	148,225	1,330,947	1,182,722	442,368	1,625,090

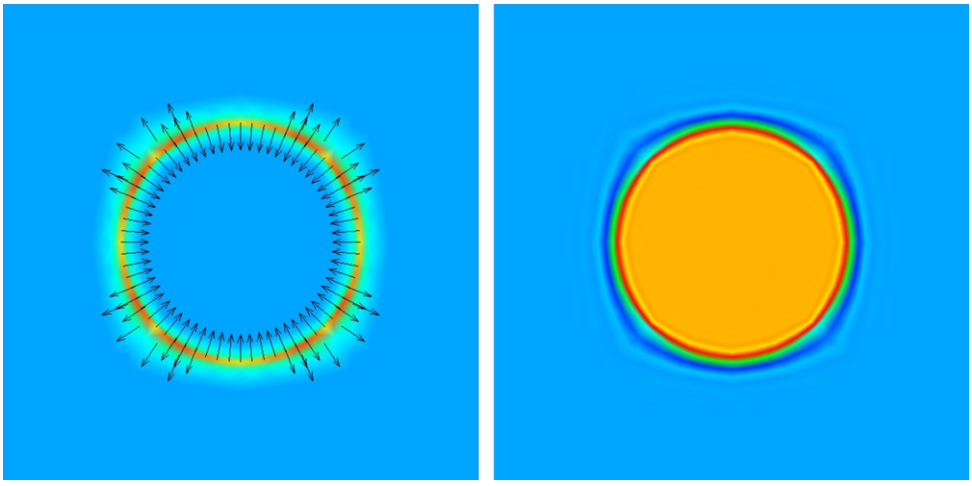

Fig. 3. Spurious velocity (left) and pressure (right) in case 1.

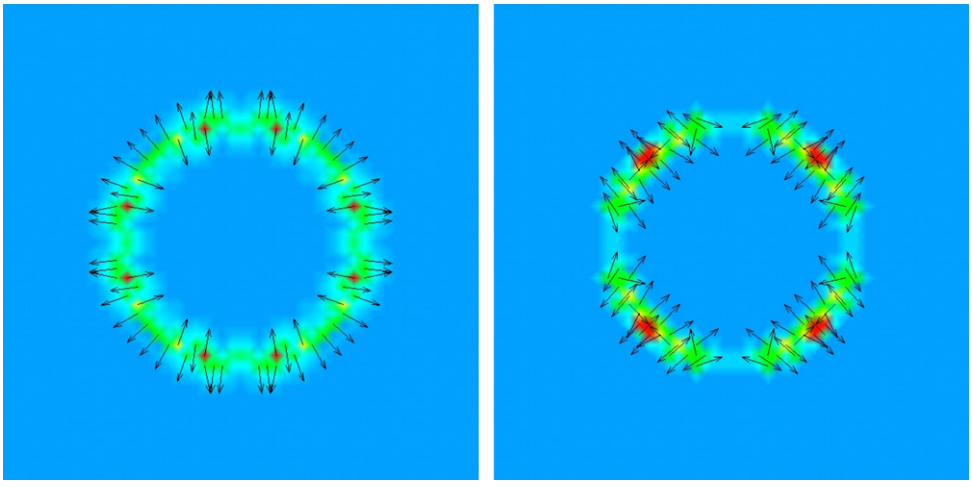

Fig. 4. Spurious velocities in case 2 (left) and case 3 (right).

velocities occur due to the continuous pressure approximation which is not capable to catch the pressure jump on the interface Γ_F, see Fig. 3. The results for the case 0 are not presented here since the velocity is numerically zero for this case, i.e., no spurious velocities are generated.

The velocity error in the L^2-norm and the obtained order of convergence for the cases 1–3 are presented in Fig. 5. The velocity error in the H^1-semi norm together with the corresponding convergence order is shown in Fig. 6. Furthermore, Fig. 7 gives the pressure error in the L^2-norm and the associated order of convergence. The velocity errors in the cases 1 and 2 (continuous pressure approximation) are slightly larger in comparison to case 3 (discontinuous pressure approximation on non-adapted meshes). An interesting observation is that the velocity error in case 1 (interface is resolved) is not better than in the cases 2 and 3. Among these three considered cases, the velocity error in case 3 (discontinuous pressure approximation on non-adapted meshes) is considerably smaller. But among all considered cases, the case 0 gives the best result which is almost exact. Since the curvature term is handled exactly here, the only source for a velocity error is the approximation property of the pressure space, compare (6). In the previous section we have shown that the error for the best approximation of discontinuous functions is of order $\mathcal{O}(\sqrt{h})$ in the cases 1–3. Using (6), this gives also a convergence order of 1/2 in the H^1-semi norm for the velocity. This is confirmed by our numerical results, see the right picture in Fig. 6.

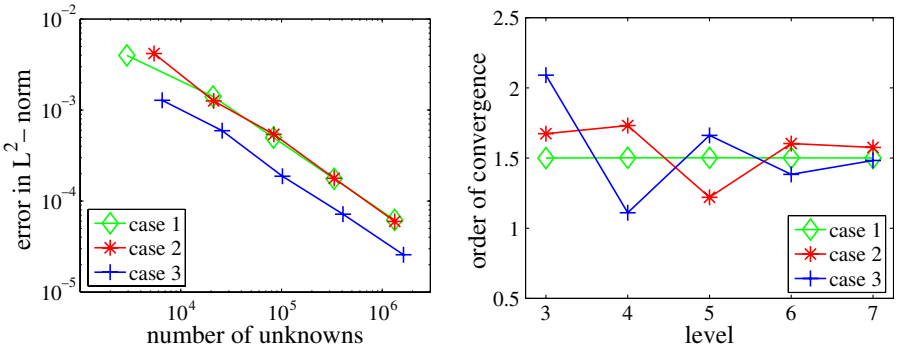

Fig. 5. Velocity error in L^2-norm (left) and rate of convergence (right).

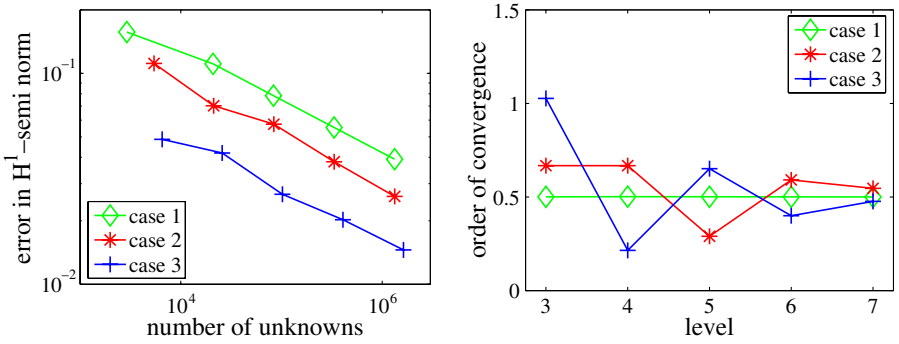

Fig. 6. Velocity error in H^1-semi norm (left) and convergence order (right).

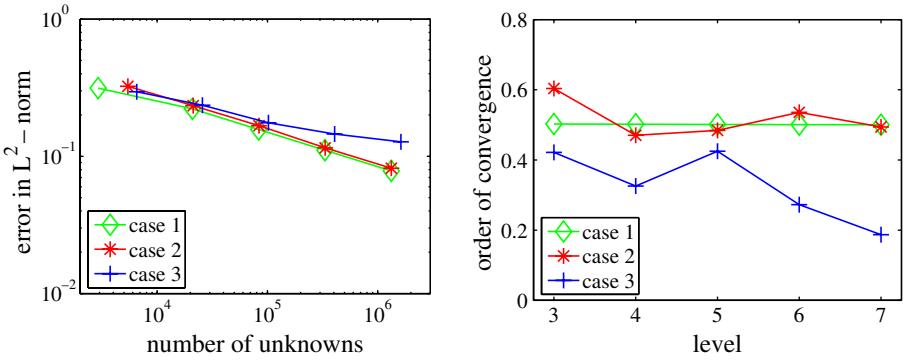

Fig. 7. Pressure error in L^2-norm (left) and convergence order (right).

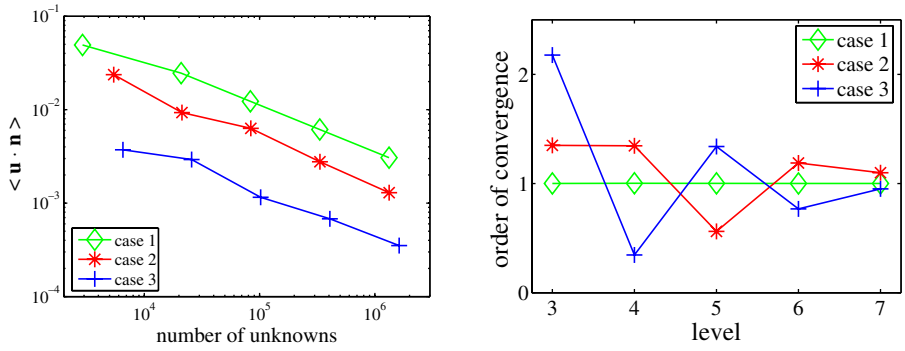

Fig. 8. Modulus of the normal flux through the interface Γ_F (left) and order of reduction (right).

4.2. Normal flux at the interface

Applying the divergence theorem to the domain Ω_1, we get from the incompressibility constraint in Eq. (1) a zero normal flux on the interface Γ_F. In order to check this condition also for the obtained discrete velocities, we calculate the discrete normal fluxes for all four considered cases. Since there are no spurious velocities in case 0, the normal flux is numerically zero. The discrete normal fluxes for the cases 1–3 are presented in Fig. 8. The normal flux for the case 1 is larger than for the cases 2 and 3. Case 2 behaves slightly better than case 1 but the case 3 (discontinuous pressure approximation on non-adapted meshes) is roughly one order of magnitude better than the case 1.

4.3. Influence of curvature handling techniques on spurious velocity for non-isoparametric and isoparametric elements

For the considered problem, the discontinuous pressure approximation on interface adapted meshes gives the best results. Now, we want to study the influence of the boundary representation. To this end, we consider bilinear (non-isoparametric) and the isoparametric reference mappings. The corresponding discretisations are denoted by Q_2/P_1^{disc} and $iso - Q_2/P_1^{\text{disc}}$.

To study the influence of the curvature approximation on both the bilinear and isoparametric discretisations, we consider the following three variants

var 0: given curvature $\kappa = 1$,
var 1: calculating the curvature from the interpolated cubic splines,
var 2: integration by parts of the Laplace–Beltrami operator,

which are described in Section 2.2. As discussed earlier, the velocity error for both the bilinear and isoparametric cases of variant 0 is numerically zero and hence not presented here. The velocity error in the L^2-norm and the associated order of convergence for the variants 1 and 2 for both the bilinear and isoparametric cases are presented in Fig. 9. The velocity error in the H^1-semi norm and the obtained order of convergence are presented in Fig. 10. For the bilinear case, variant 2 (integration by parts in Laplace–Beltrami operator) gives in comparison with variant 1 (interpolated cubic spline) much larger velocity errors in both the L^2-norm and the H^1-semi norm, see left pictures in Figs. 9 and 10. Furthermore, the convergence orders for variant 2 are always 2 smaller than the orders for variant 1, see right pictures in Figs. 9 and 10. In the H^1-semi norm, the convergence order reduces to 1/2, see Fig. 10. The only reason for this bad behaviour is the poor approximation of the curvature term since the pressure approximation is sufficiently good, see (6). However, for the isoparametric case the velocity errors in the variants 1 and 2 are similar and the convergence orders are same for both the variants. These numerical results indicate that

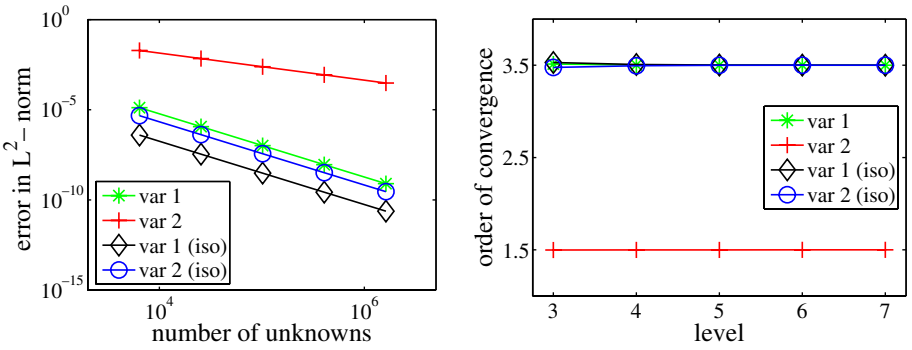

Fig. 9. Velocity error in L^2-norm (left) and convergence order (right) on adapted meshes for non-isoparametric and isoparametric elements.

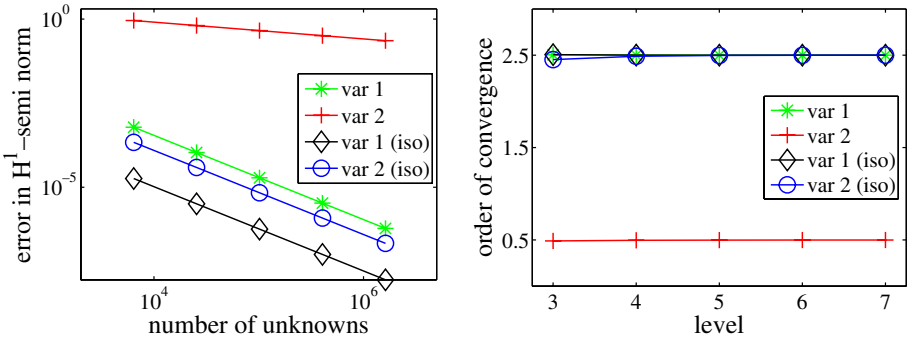

Fig. 10. Velocity error in H^1-semi norm (left) and convergence order (right) on adapted meshes for non-isoparametric and isoparametric elements.

any of the considered variants can be used for the isoparametric case but for the non-isoparametric case the variant 1 which is based on the interpolated cubic spline should be preferred.

5. Conclusions

The solutions of two-phase flow problems exhibit in general reduced regularity properties across the interface. This may lead to a reduction of convergence order when the mesh does not resolve the interface. That this really happens has been demonstrated in the one-dimensional case analytically by studying the best approximation of a discontinuous function in L^2. In the two-dimensional case we see this reduction effect numerically for a two-phase model problem. Moreover, we have shown that for continuous, piecewise linear pressure approximations the interface resolution by the mesh is not sufficient to get the expected convergence orders. Discontinuous, piecewise linear pressure approximations on interface adapted meshes behave much better, they show the expected convergence order: in our model problem the error is practically zero. If the interface is not sufficiently resolved by the mesh then the convergence order of discontinuous, piecewise linear approximations reduces from two to one-half.

Since our discrete solutions are only discretely divergence-free but not divergence-free, spurious velocities are observed which are mainly concentrated in the neighbourhood of the interface. This leads to a non-zero flux at the interface although our test example has zero flux along the interface. Note that the precise calculation of the velocity field close to the interface is extremely important in moving free boundary problems. Indeed, in the ALE (Arbitrary Lagrangian–Eulerian) approach the position of the free boundary at the next time step is determined from the kinematic condition that the normal velocity of the boundary is equal to the normal component of the fluid velocity. When using a level set method, the movement of the level set function depends strongly on the approximated velocity field. Thus, spurious velocities should be as small as possible.

For suppressing spurious velocities caused by the discretisation of local external forces two aspects are important: the accurate approximation of the curvature and the free boundary. For a given external force (curvature $\mathscr{K} = 1$) we practically do not observe any error independent of taking non-isoparametric or isoparametric finite elements. However, in practise one has to find the external forces as parts of the problem. Then, the calculation of the curvature from a cubic spline approximation of the free boundary works well in both the non-isoparametric and isoparametric case. However, the Laplace–Beltrami approach requires the use of isoparametric finite elements to avoid a drastic reduction of the convergence order.

Summarising, in two-phase flows we recommend to use discontinuous pressure approximations and isoparametric finite elements of higher (at least second) order to approximate the interface. In the two-dimensional case, the handling of the curvature seems to be a matter of taste because the cubic spline approximation of the free boundary requires only the solution of a tridiagonal system of linear equations. However, in the three-dimensional case, the introduction of the Laplace–Beltrami operator could be advantageous.

References

[1] P. Gresho, R. Lee, S. Chan, J. Leone, A new finite element for incompressible or Boussinesq fluids, in: Proc. Third Int. Conf. on Finite Elements in Flow Problems, Banff, Canada, 1980, pp. 204–215.
[2] D. Pelletier, A. Fortin, R. Camarero, Are FEM solutions of incompressible flows really incompressible? (Or how simple flows can cause headaches!), Int. J. Numer. Methods Fluids 9 (1989) 99–112.
[3] O. Dorok, Eine stabilisierte Finite-Elemente-Methode zur Lösung der Boussinesq-Approximation der Navier-Stokes-Gleichungen, Ph.D. thesis, Otto-von-Guericke-Universität (1995).
[4] J.-F. Gerbeau, C. le Bris, M. Bercovier, Spurious velocities in the steady flow of an incompressible fluid subjected to external forces, Int. J. Numer. Methods Fluids 25 (1997) 679–695.
[5] B. Lafaurie, C. Nardone, R. Scardovelli, S. Zaleski, G. Zanetti, Modelling merging and fragmentation in multiphase flows with SURFER, J. Comput. Phys. 113 (1994) 134–147.
[6] M. Fortin, A. Fortin, Experiments with several elements for viscous incompressible flows, Int. J. Numer. Methods Fluids 5 (1985) 911–928.
[7] O. Dorok, W. Grambow, L. Tobiska, Aspects of finite element discretizations for solving the Boussinesq approximation of the Navier–Stokes equations., in: F.-K. Hebeker, R. Rannacher, G. Wittum (Eds.), Numerical Methods for the Navier–Stokes Equations.

Notes on Numerical Fluid Mechanics, vol. 47. Proceedings of the International Workshop held at Heidelberg, October 25–28, 1993, Vieweg, Braunschweig, 1994, pp. 50–61.

[8] S. Ganesan, V. John, Pressure separation – a technique for improving the velocity error in finite element discretisations of the Navier–Stokes equations, Appl. Math. Comp. 165 (2005) 275–290.

[9] V. Girault, P.-A. Raviart, Finite Element Methods for Navier–Stokes equations, Springer-Verlag, Berlin, Heidelberg, New York, 1986.

[10] G. Matthies, L. Tobiska, The Inf–Sup Condition for the Mapped $Q_k/P_{k-1}^{\mathrm{disc}}$ element in arbitrary space dimensions, Computing 69 (2) (2002) 119–139.

[11] K. Ruschak, A method for incorporating free boundaries with surface tension in finite element fluid-flow simulators, Int. J. Numer. Meth. Engng. 15 (1980) 639–648.

[12] G. Dziuk, Finite elements for the Beltrami operator on arbitrary surfaces, in: S. Hildebrandt, R. Leis (Eds.), Partial Differential Equations and Calculus of Variations, Springer, Berlin, 1988, pp. 142–155.

[13] G. Dziuk, An algorithm for evolutionary surfaces, Numer. Math. 58 (6) (1991) 603–611.

[14] E. Bänsch, Numerical methods for the instationary Navier–Stokes equations with a free capillary surface, Habilitationsschrift, Albert-Ludwigs-Universität, Freiburg i. Br., 1998.

[15] E. Bänsch, Finite element discretization of the Navier–Stokes equations with a free capillary surface, Numer. Math. 88 (2) (2001) 203–235.

[16] D. Gilbarg, N.S. Trudinger, Elliptic partial differential equations of second order, Springer-Verlag, Berlin, 2001, reprint of the 1998 edition.

[17] V. John, P. Knobloch, G. Matthies, L. Tobiska, Non-nested multi-level solvers for finite element discretisations of mixed problems, Computing 68 (4) (2002) 313–341.

[18] V. John, G. Matthies, MooNMD – a program package based on mapped finite element methods, Comput. Vis. Sci. 6 (2–3) (2004) 163–170.